

# Formation of a Syndiotactic Organic Polymer Inside a MOF by a [2+2] Photo-Polymerization Reaction\*\*

In-Hyeok Park, Raghavender Medishetty, Hyeong-Hwan Lee, Caroline Evania Mulijanto, Hong Sheng Quah, Shim Sung Lee,\* and Jagadeese J. Vittal\*

**Abstract:** Getting suitable crystals for single-crystal X-ray crystallographic analysis still remains an art. Obtaining single crystals of metal–organic frameworks (MOFs) containing organic polymers poses even greater challenges. Here we demonstrate the formation of a syndiotactic organic polymer ligand inside a MOF by quantitative [2+2] photopolymerization reaction in a single-crystal-to-single-crystal manner. The spacer ligands with *trans,trans,trans*-conformation in the pillared-layer MOF with guest water molecules in the channels, undergo pedal motion to *trans,cis,trans*-conformation prior to [2+2] photo-cycloaddition reaction and yield single crystals of MOF containing two-dimensional coordination polymers fused with the organic polymer ligands. We also show that the organic polymer in the single crystals can be depolymerized reversibly by cleaving the cyclobutane rings upon heating. These MOFs also show interesting photoluminescent properties and sensing of small organic molecules.

Growing good quality crystals is important in determining the three-dimensional (3D) arrangements of atoms and molecules in the solid state by single-crystal X-ray diffraction (SC-XRD) techniques. Understanding of the crystal packing enables us to explore the structure–property relationship for creating new advanced solid-state materials.<sup>[1]</sup> Crystalline properties arising from the orderly arrangements of polymer chains are well-sought to control mechanical, chemical, optical, and electrical properties for various industrial applications.<sup>[2]</sup> The tactic polymers, on the contrary, display a high degree of crystallinity and are usually synthesized in solution using metal catalysts.<sup>[3]</sup> Topochemical polymerization reactions have been used to make a number of highly crystalline organic polymers in the solid state, but making tactic polymers by a solid-state route is elusive.<sup>[4]</sup> Recently, an isotactic polymer ligand embedded inside single crystals of

metal–organic frameworks (MOFs) was made through polymerization of a well-aligned slip-stacked conjugated diene ligand 1,4-bis[2-(4'-pyridyl)ethenyl]benzene (bpeb) by [2+2] cycloaddition reaction under UV light.<sup>[5]</sup> Here we report the formation of a syndiotactic polymer ligand (shown in Figure 1) incorporated inside another MOF through single-

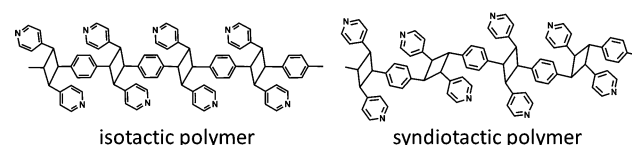


**Figure 1.** Structural diagrams of the two tactic polymers from the solid-state [2+2] photopolymerization of bpeb ligand.

crystal-to-single-crystal (SCSC) reaction, but the unexpected photoreaction could not be predicted from the crystal packing. In the pillared-layer MOF accommodating guest water molecules in the channels, the spacer ligands undergo pedal motion under UV light prior to photoreaction to meet Schmidt's criteria for [2+2] cycloaddition reaction. As a result, single crystals of MOF containing a 2D coordination polymer (CP) integrated with the syndiotactic organic polymeric ligand were obtained in an SCSC fashion. The organic polymer in the single crystals can be depolymerized reversibly by cleaving the cyclobutane rings upon heating.

A three-fold interpenetrated pillared-layer MOF with **pcu** topology,  $[\text{Zn}_2(\text{bpeb})(\text{obc})_2] \cdot 2\text{DMF} \cdot \text{H}_2\text{O}$  [**1**;  $\text{H}_2\text{obc} = 4,4'$ -oxybis(benzoic acid)] has been shown to retain its single crystal nature when the guest solvents were exchanged in methanol to form **2**.<sup>[6]</sup> Both **1** and **2** were found to be photo-inactive as the olefin bonds in bpeb ligands were separated by  $>4.2 \text{ \AA}$ . The guest solvents could be removed without destroying its single crystallinity by heating **2** at  $160^\circ\text{C}$  for 6 h, but on standing in air, it takes water from humid air to form  $[\text{Zn}_2(\text{bpeb})(\text{obc})_2] \cdot 4\text{H}_2\text{O}$  (**3**) as shown by SC-XRD studies.

The asymmetric unit of **3** contains a molecular formula unit. Each  $\text{Zn}^{\text{II}}$  is bridged by two obc ligands and chelated to another obc ligand (Figure 2a). The highly distorted dimer unit extends through these four obc ligands and forms a layer structure (Figure 2b). The highly corrugated (4,4) layers of  $[\text{Zn}_2(\text{obc})_2]$  with honeycomb-like cavity are pillared by the bpeb ligands forming a pillared-layer structure as shown in Figure 2c. The two pyridyl rings in the bpeb ligand are twisted with respect to the middle ring by  $20.3^\circ$  and  $31.0^\circ$  and the ligand has *trans,trans,trans*-conformation. The overall topology of the 3D structure is a **pcu** net. The large void

[\*] Dr. I.-H. Park, H.-H. Lee, Prof. S. S. Lee  
Department of Chemistry and Research Institute of Natural Science  
Gyeongsang National University  
Jinju 660-701 (Republic of Korea)  
E-mail: sslee@gnu.ac.kr

Dr. R. Medishetty, C. E. Mulijanto, H. S. Quah, Prof. J. J. Vittal  
Department of Chemistry, National University of Singapore  
3, Science Drive 3, Singapore 117543 (Singapore)  
E-mail: chmjv@nus.edu.sg

[\*\*] This work was supported by the NRF (2012R1A4A1027750), S. Korea, and the Ministry of Education, Singapore through NUS FRC grant R-143-000-562-112. Dr. Srinivasulu Aitipamula of ICES is thanked for the pharmaceutical samples tested in the manuscript.

Supporting information for this article is available on the WWW under <http://dx.doi.org/10.1002/anie.201502179>.

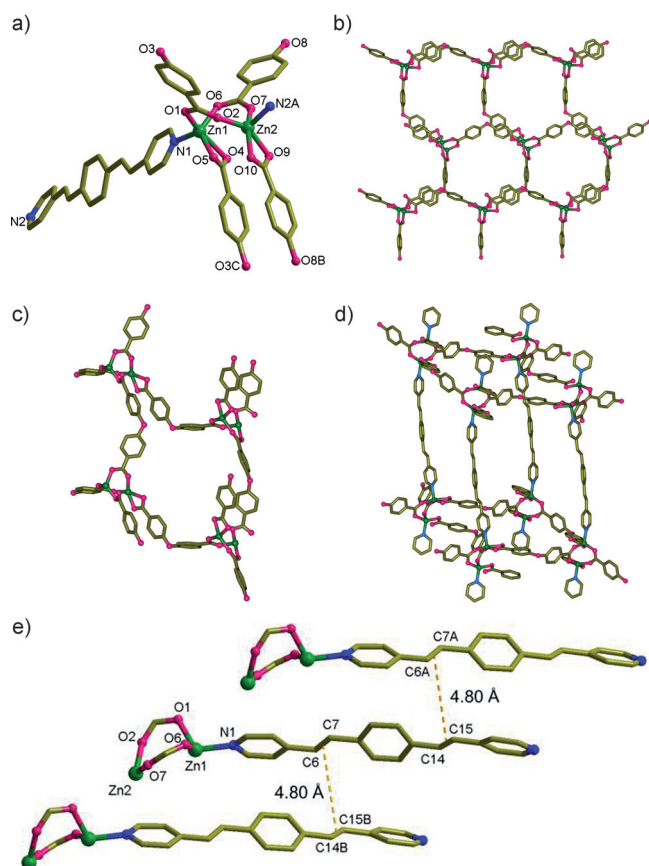


**Figure 2.** a) Building block of **3**. The disorder in one obc is not shown. b) Highly corrugated (4,4) layer formed by  $[\text{Zn}_2(\text{obc})_2]$ . c) A single ring in the (4,4) net. d) A single primitive cube. e) A view of the packing showing the crisscrossed alignment of bpeb ligands. Symmetry codes: A)  $x, 0.5 - y, 0.5 + z$ ; B)  $x, 0.5 - y, -0.5 + z$ .

generated by the long spacer ligand was filled by three-fold interpenetration. The total potential solvent area volume as calculated by PLATON<sup>[7]</sup> in **3** is 881.9 Å<sup>3</sup> which is 18.6% of the unit cell volume 4733.4 Å<sup>3</sup>. The empty space is occupied by highly disordered water molecules. Overall, **3** is isotypical to **2**.

The bpeb ligands from the neighboring **pcu** units in **3** are disposed in slip-stacked manner but the olefin bonds are crisscrossed with respect to each other and separated by 4.8 Å (Figure 2d). Surprisingly, irradiation of the pale yellow crystals of **3** under a Xe-lamp of wavelength 365 nm for 2 h resulted in shattering of the single crystals and yielded  $[\text{Zn}_2(S\text{-poly-bppcb})_{0.5}(\text{obc})_2] \cdot 2.5\text{H}_2\text{O}$  (**4**) in which *S*-poly-bppcb is syndiotactic-1,3-(4,4'-bipyridyl)-2-phenylcyclobutane polymer. Characterization by solution <sup>1</sup>H NMR spectroscopy was not possible due to its insolubility even in strong acids, indirectly inferring the formation of the organic polymer. Fortunately, the crystals from the shattered big crystals were suitable for data collection.

The formation of the polymer ligand in **4** by the [2+2] cycloaddition reaction was established by single-crystal X-ray crystallography. Interestingly, the space group *P*2<sub>1</sub>/*c* was retained in this reaction, but the volume of the unit cell was reduced from 4733.4(4) Å<sup>3</sup> to 4651.7(9) Å<sup>3</sup>. The asymmetric

unit in **4** consists of a formula unit. Unlike **3**, one carboxylate oxygen atom (O4) chelated to Zn1 in **4** strongly binds to Zn2 with a distance of 2.325(6) Å to provide the coordination of Zn2 from a distorted square pyramidal geometry in **3** to a distorted octahedral geometry in **4** (Figure S15). Although Zn1 in **4** still has a highly distorted 5-coordinate geometry as shown in Figure 3a and  $[\text{Zn}_2(\text{obc})_2]$  forms a similar corrugated (4,4) sheet structure (Figure 3b), the photopolymerized product *S*-poly-bppcb has been found to be integrated into this MOF (Figure 3c).

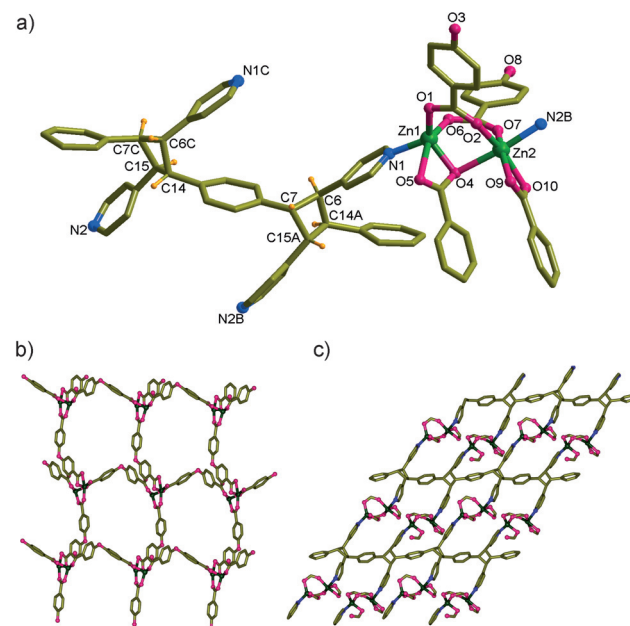


**Figure 3.** Structure of **4**,  $[\text{Zn}_2(S\text{-poly-bppcb})_{0.5}(\text{obc})_2] \cdot 2.5\text{H}_2\text{O}$ . a) A view showing the coordination environment of  $\text{Zn}^{\text{II}}$  atoms. Symmetry codes: A)  $x, 1.5 - y, -0.5 + z$ ; B)  $-1 + x, 1.5 - y, -1.5 + z$ ; C)  $x, 1.5 - y, 0.5 + z$ . b) The (4,4) layer formed by  $[\text{Zn}_2(\text{obc})_2]$  connectivity. c) The 2D layer formed by  $[\text{Zn}_2(S\text{-poly-bppcb})_{0.5}(\text{O}_2\text{C-C})_4]$  moiety.

The cyclobutane rings in **4** unite all the bpeb pillars in the former three-fold interpenetrated structure (**3**). Thus, incorporation of the new organic polymer ligand with the  $[\text{Zn}_2(\text{obc})_2]$  sheet results in a 3D structure without interpenetration. This unusual binodal net constructed from the infinite square planar nodes created by the cyclobutane rings of the *S*-poly-bppcb ligand, and the tetrahedral nodes of  $\text{Zn}^{\text{II}}$  atoms give rise to a new (4,4) connected net which we call *jjv*3 with a point symbol  $\{4^4.5^2.6^9\}\{5^3.6^3\}$  4,6-*c* net with stoichiometry (4-*c*)(6-*c*); two-nodal net transitivity [24] self catenated as shown in Figure 4.<sup>[8]</sup>

The *S*-poly-bppcb ligand is a syndiotactic polymer whereas the polymer obtained recently from another solid-state reaction is isotactic (Figures 1 and 5).<sup>[5]</sup> Indeed, the isotactic polymer was obtained from a [2+2] cycloaddition reaction between perfectly well-aligned olefin bonds among slip-stacked arrangements of *trans,trans,trans*-bpeb ligands. However, the *S*-poly-bppcb ligand in **4** could have formed only by the polymerization of the *trans,cis,trans*-bpeb ligands (Figure S14). Nonetheless the crystal structure revealed the conformation of the bpeb ligand in **3** to be all *trans*. It was

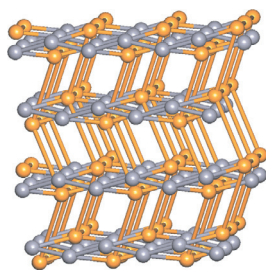


**Figure 4.** A view of the non-interpenetrated net,  $jju3$  in **4** viewed along the  $a$ -axis. The topological representation of the 3D framework created from 2D sheets formed from the tetrahedral Zn1 node (golden yellow) and  $S$ -poly-bppcb node (gray) through obc spacer ligand (golden yellow rod).

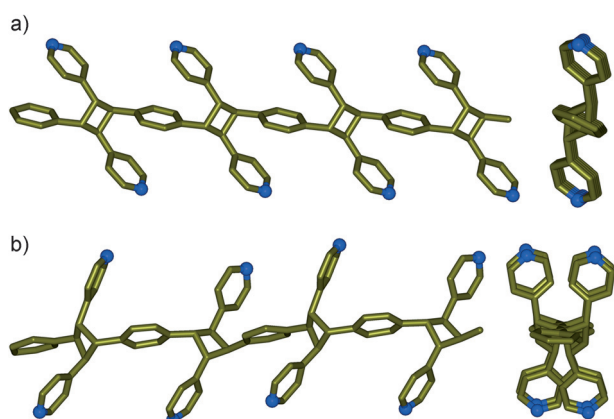


**Figure 5.** The isotactic and the syndiotactic polymers. a) Two views of the isotactic polymer described in Ref. [5]. b) The syndiotactic polymer in **4** from this work.

realized that Schmidt's criteria were not met in **3** to be photoreactive. The very fact that **3** is photoreactive and the formation of  $S$ -poly-bppcb ligand in **4** is unequivocally characterized in the solid state, this observation has been rationalized as follows. The *trans,trans,trans*-bpeb ligand in **3** undergoes pedal motion to form the *trans,cis,trans*-conformation as a transition state under UV light and the change in the conformation of bpeb brought the olefin bonds closer together within 4.2 Å in the parallel alignment for the photoreaction to occur. Unexpected photoreactivity in organic crystals is nothing new and has been observed before.<sup>[9]</sup>

The crystal structures of **2** and **3** are isomorphous and isostructural. There is little difference in their repeating units and packing (Figure S10) and hence the difference in their photoreactivity behavior could not be explained in terms of the metric parameters of these structures. Surprisingly **3** was found to be photoreactive but not **2** which was obtained from **1** by exchanging with methanol. Further, thermogravimetry-mass spectrometry (TG-MS) studies of **2** show the presence of methanol solvates and no water in the channel. The composition of **2** has been redetermined to be  $[\text{Zn}_2(\text{bpeb})(\text{obc})_2] \cdot 2 \text{ MeOH}$  from the  $^1\text{H NMR}$  and TG-MS data. We have noticed that the single crystals of **1–4** are quite robust to the exchange and removal of solvents. For example, photo-

reactive **3** could be obtained by heating the single crystals of **1** at 160 °C for 6 h. It is likely that the presence of methanol or DMF guest molecules in the channels hinders photoreactivity in **1** and **2**, whereas water alone in the channel promotes pedal motion and hence the photoreactivity. The interactions between the solvents and the organic ligands (chromophores) are known to alter the intensity and their emission wavelengths of photoluminescent MOFs.<sup>[10]</sup> Based on these observations, it is concluded that the interactions with solvents can also alter the pedal motion in these MOFs. However, such influence of solvents on the pedal motion which resulted in photoreactivity observed in this work, to the best of our knowledge, has never been documented before.<sup>[11]</sup>

Since **4** is thermally stable up to 350 °C, thermal cleavage of the cyclobutane rings in the organic polymer was attempted. When the single crystals of **4** were heated to 250 °C for 3 h in a hot air oven, the pale yellow crystals became light brown crystals (**3a**) with some cracks which were cut later and used for single-crystal X-ray intensity data collection. The solid-state structure determination of the heated sample **3a** by X-ray crystallography showed that depolymerization occurred due to the cleavage of the cyclobutane rings in the  $S$ -poly-bppcb ligand. Interestingly, the water vapors were also absorbed back to the empty voids in **3a**.

The solid-state photoluminescence (PL) spectra of **1–3** show different  $\lambda_{\text{max}}$  at 473, 444, and 504 nm, respectively, when excited at 360 nm and the intensities are much stronger than bpeb and  $\text{H}_2\text{obc}$  ligands (Figure S19). This is expected due to the presence of different solvents in the lattice.<sup>[10]</sup> However, when they were dispersed in DMF, the  $\lambda_{\text{max}}$  occurs around 420–430 nm due to the exchange of solvents by DMF (Figure S21). Further, the PL of **4** shows quite broad and stronger emission at 415 nm with shoulders at 397 and 435 nm. Due to these emissive properties, **1–4** were tested for sensing some of the available common drug molecules and nitro derivatives (Figures 6, S30, and S31). Interestingly, curcumin has the ability to quench the PL intensities of **1–4** and **4** is able to detect the presence of curcumin up to 1 ppm in DMF solution (Figure S25). Furthermore, **4** shows selective sensing for flufenamic acid (i.e., 2-[[3-(trifluoromethyl)phenyl]amino]benzoic acid, a nonsteroidal antiinflammatory drug) and indometacin (2-[1-[(4-chlorophenyl)carbonyl]-5-methoxy-2-methyl-1*H*-indol-3-yl]acetic acid, a nonsteroidal antiinflammatory drug) among 16 different drug molecules tested (Figures 6a and S30). Compounds **1–4** also show selective sensing of 2,4-dinitrophenol, 4-nitroaniline, and 2,4-dinitrophenylhydrazine (Brady's reagent) among ten different nitro organic molecules investigated (Figures 6b and S31).

In this work, the solid-state [2+2] cycloaddition reaction has been used to synthesize a syndiotactic organic polymer ligand incorporated in a MOF structure (**4**) in an SCSC manner, through slip-stacked arrangement of the bpeb ligands. Although both parallel alignment and distance criterion delineated by Schmidt were not met for bpeb ligands, **3** has been found to undergo [2+2] cycloaddition reaction quantitatively under UV light to form **4**. The all-*trans* conformation of the bpeb ligand isomerized to *trans,cis,trans*



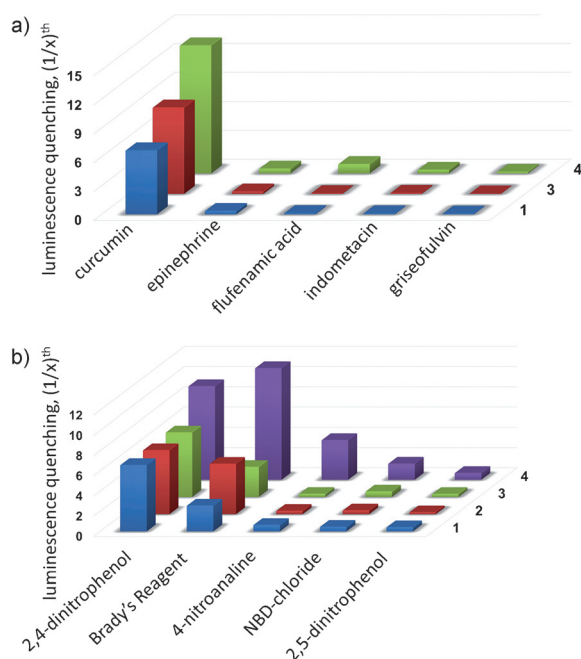


**Figure 6.** PL quenching efficiencies ( $I_0/I-1$ ) obtained from a) selected drug analytes **1**, **3**, and **4** and b) selected nitro analytes **1–4**.

conformation by pedal motion prior to photoreaction under UV light. Due to this conformational change, the olefin bonds in the bpeb ligands are drawn closer together to facilitate the polymerization reaction forming a syndiotactic polymer (Figure 7).

In the solids containing photoreactive ligand, the olefin bond pairs have been found to undergo crisscross to parallel

obtained isotactic organic polymer.<sup>[5]</sup> Although the usefulness of these highly tactic organic polymer ligand is yet to be realized, the solid-state photopolymerization reaction observed here opens up a new opportunity to generate highly crystalline MOFs containing tactic organic polymers, which may not be directly accessible by the traditional solution route. In **4** both the *S*-poly-bppcb ligand and  $\text{Zn}_2(\text{obc})_2$  CP are integrated into a 3D architecture with a new topology. Further, the cyclobutane in **4** can be cleaved back to all-*trans*-bpeb ligand to form **3** reversibly in an SCSC fashion by heating, similar to that observed in isotactic polymer.<sup>[5]</sup> Such a rare depolymerization reaction is probably possible due to the very high thermal stability of **4**.

Both crystals of **2** and **3** are isostructural but differ in having different guest solvents in the channels. Indeed, **2** can be converted to **3** in an SCSC manner. It is rather surprising that the absence of methanol/DMF or the presence of water in the channel makes **3** to undergo pedal motion and hence amenable to photoreaction. Such an influence of the guest molecules in channel on the pedal motion and its subsequent photoreactivity of MOFs underpin the unknown factors beyond Schmidt's rule in solid-state photoreactivity.<sup>[9a–c]</sup>

Although **1–3** display varied solid-state emissive properties due to the presence of different solvents in the channels, they show the same behavior in the dispersed DMF solution, as the solvents are exchanged with DMF eventually. Preferential quenching of PL emissions of **2–4** by curcumin, 2,4-dinitrophenol, and 2,4-dinitrophenylhydrazine makes them potentially useful sensing agents.

CCDC 1044537 (**3**), 1044538 (**3a**), 1044539 (**3b**), 1044540 (**4**) contain the supplementary crystallographic data for this paper. These data can be obtained free of charge from The Cambridge Crystallographic Data Centre via [www.ccdc.cam.ac.uk/data\\_request/cif](http://www.ccdc.cam.ac.uk/data_request/cif).

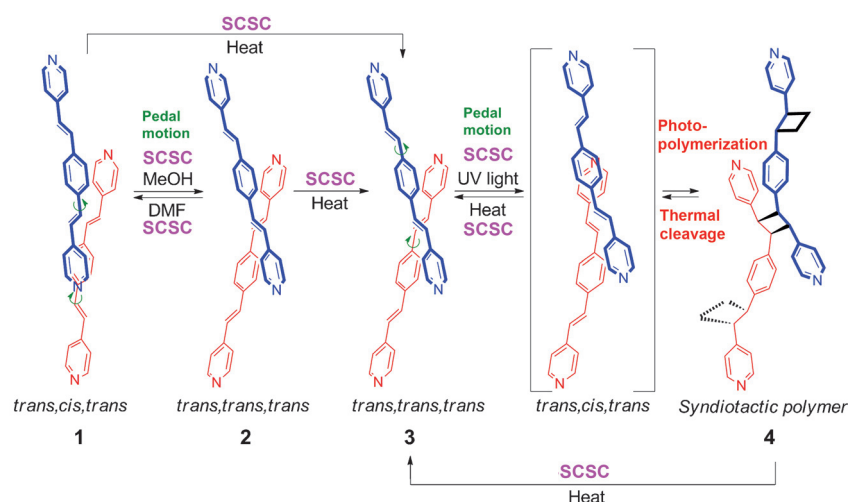


**Figure 7.** A schematic diagram illustrating various SCSC conversions among **1–4** involving bpeb ligands.

orientations to form the usually expected *rcctt*-isomer (*rcctt* = *region-cis,trans,trans*) of the cyclobutane ring.<sup>[4b,11]</sup> In the case of **3**, pedal motion orchestrated the creation of a syndiotactic organic polymer which is different from the previously

## Experimental Section

$[\text{Zn}_2(\text{bpeb})(\text{obc})_2] \cdot 2\text{DMF} \cdot \text{H}_2\text{O}$  (**1**) and  $[\text{Zn}_2(\text{bpeb})(\text{obc})_2] \cdot 2\text{MeOH}$  (**2**): The single crystals of **1** and **2** were synthesized according to a reported procedure.<sup>[6]</sup>

$[\text{Zn}_2(\text{bpeb})(\text{obc})_2] \cdot 4\text{H}_2\text{O}$  (**3**): The single crystals of **2** were heated to 160 °C in a hot air oven. After 6 h, yellow crystals of **3** suitable for X-ray analysis were obtained.

$[\text{Zn}_2(\text{S-poly-bppcb})(\text{obc})_2] \cdot 2.5\text{H}_2\text{O}$  (**4**): The yellowish white plate-shaped crystals of **4** were obtained by UV irradiation of single crystals of **3** for 2 h.

$[\text{Zn}_2(\text{bpeb})(\text{obc})_2] \cdot 3\text{H}_2\text{O}$  (**3a**): The single crystals of **4** were heated to 250 °C in a hot air oven. After 3 h, the light yellow crystals of **3a** suitable for X-ray analysis were obtained.

$[\text{Zn}_2(\text{bpeb})(\text{obc})_2] \cdot 4\text{H}_2\text{O}$  (**3b**): The single crystals of **1** were heated to 160 °C in a hot air oven. After 6 h, yellow crystals of **3b** suitable for X-ray analysis were obtained.

**Keywords:** [2+2] cycloaddition · metal–organic frameworks · pedal motion · sensors · syndiotactic polymers

**How to cite:** *Angew. Chem. Int. Ed.* **2015**, *54*, 7313–7317  
*Angew. Chem.* **2015**, *127*, 7421–7425

- 
- [1] a) E. M. Landau, M. Levanon, L. Leiserowitz, M. Lahav, J. Sagiv, *Nature* **1985**, *318*, 353–356; b) Y. Yin, R. M. Rioux, C. K. Erdonmez, S. Hughes, G. A. Somorjai, A. P. Alivisatos, *Science* **2004**, *304*, 711–714; c) S. Mann, G. A. Ozin, *Nature* **1996**, *382*, 313–318.
- [2] a) G. Lamberti, *Chem. Soc. Rev.* **2014**, *43*, 2240–2252; b) T. Nakano, Y. Okamoto, *Chem. Rev.* **2001**, *101*, 4013–4038.
- [3] a) W. Kaminsky, *Macromol. Chem. Phys.* **1996**, *197*, 3907–3945; b) N. Ishihara, M. Kuramoto, M. Uoi, *Macromolecules* **1988**, *21*, 3356–3360; c) B. M. Chamberlain, M. Cheng, D. R. Moore, T. M. Ovitt, E. B. Lobkovsky, G. W. Coates, *J. Am. Chem. Soc.* **2001**, *123*, 3229–3238.
- [4] a) J. W. Lauher, F. W. Fowler, N. S. Goroff, *Acc. Chem. Res.* **2008**, *41*, 1215–1229; b) Y. Sonoda, *Molecules* **2011**, *16*, 119–148; c) G. W. Goodall, W. Hayes, *Chem. Soc. Rev.* **2006**, *35*, 280–312; d) M. Hasegawa, *Chem. Rev.* **1983**, *83*, 507–518.
- [5] I.-H. Park, A. Chanthapally, Z. Zhang, S. S. Lee, M. J. Zaworotko, J. J. Vittal, *Angew. Chem. Int. Ed.* **2014**, *53*, 414–419; *Angew. Chem.* **2014**, *126*, 424–429.
- [6] I.-H. Park, S. S. Lee, J. J. Vittal, *Chem. Eur. J.* **2013**, *19*, 2695–2702.
- [7] A. L. Spek. PLATON, A Multipurpose Crystallographic Tool, University of Utrecht, Utrecht, The Netherlands. **2003**.
- [8] a) V. A. Blatov, *Struct. Chem.* **2012**, *23*, 955–963; b) V. A. Blatov, *IUCr Comp. Comm. News. Lett.* **2006**, *7*, 4; c) E. V. Alexandrov, V. A. Blatov, A. V. Kochetkov, D. M. Proserpio, *CrystEngComm* **2011**, *13*, 3947–3958.
- [9] a) G. Kaupp, *Curr. Opin. Solid State Mater. Sci.* **2002**, *6*, 131–138; b) G. Kaupp, M. R. Naimi-Jamal, *CrystEngComm* **2005**, *7*, 402–410; c) G. Kaupp, E. Jostkleigrewe, H.-J. Hermann, *Angew. Chem. Int. Ed. Engl.* **1982**, *21*, 435–436; *Angew. Chem.* **1982**, *94*, 457–458; d) S. K. Kearsley, G. R. Desiraju, *Proc. R. Soc. London Ser. A* **1985**, *397*, 157–181.
- [10] a) Y. Cui, Y. Yue, G. Qian, B. Chen, *Chem. Rev.* **2012**, *112*, 1126–1162; b) M. D. Allendorf, C. A. Bauer, R. K. Bhakta, R. J. T. Houk, *Chem. Soc. Rev.* **2009**, *38*, 1330–1352; c) L. Qin, M.-X. Zheng, Z.-J. Guo, H.-G. Zheng, Y. Xu, *Chem. Commun.* **2015**, *51*, 2447–2449; d) Y. Cui, B. Chen, G. Qian, in *Metal-Organic Frameworks for Photonics Applications*, Vol. 157 (Eds.: B. Chen, G. Qian), Springer, Berlin, **2014**, pp. 27–88.
- [11] a) J. Harada, K. Ogawa, *Cryst. Growth Des.* **2014**, *14*, 5182–5188; b) J. Harada, K. Ogawa, *Chem. Soc. Rev.* **2009**, *38*, 2244–2252; c) E. Elacqua, P. Kaushik, R. H. Groeneman, J. C. Sumrak, D.-K. Bučar, L. R. MacGillivray, *Angew. Chem. Int. Ed.* **2012**, *51*, 1037–1041; *Angew. Chem.* **2012**, *124*, 1061–1065.

Received: March 8, 2015

Revised: April 13, 2015

Published online: May 7, 2015